Hindawi
Advances in Civil Engineering
Volume 2019, Article ID 1507825, 12 pages
https://doi.org/10.1155/2019/1507825

Research Article

Simplified Method for Calculating the Active Earth Pressure on Retaining Walls of Narrow Backfill Width Based on DEM Analysis

Minghui Yang[1] **and Bo Deng**[2]

[1]*Associate Professor, College of Civil Engineering, Hunan University, Changsha, Hunan 410082, China*
[2]*Ph.D. Candidate, College of Civil Engineering, Hunan University, Changsha, Hunan 410082, China*

Correspondence should be addressed to Bo Deng; parl_d@126.com

Received 22 December 2018; Revised 27 February 2019; Accepted 10 March 2019; Published 4 April 2019

Academic Editor: Victor Yepes

Spaces for backfills are often constrained and narrowed when retaining walls must be built close to existing stable walls in urban areas or near rock faces in mountainous areas. The discrete element method (DEM), using Particle Flow Code (*PFC-2D*) software, was employed to simulate the behavior of cohesionless soil with narrow width behind a rigid retaining wall when the wall translation moved away from the soils. The simulations focused on the failure model of the soil when the movement of the wall reaches the value where active earth pressure occurs, and the shape of the sliding surface was captured. Then, based on the limit equilibrium method with the obtained slip surfaces in *PFC-2D*, a simplified analytical method is presented to obtain a solution of the active earth pressure acting on rigid retaining with narrow backfill width. The point of application of the active earth pressure is also obtained. The calculated values agree well with those from physical tests in the previous literature. Furthermore, the effects of the width of the backfill, internal friction angle of soil, and wall-soil friction angle on the distribution of active earth pressure are discussed.

1. Introduction

In engineering practice, for simplification, traditional methods such as those based on the Rankine theory and Coulomb theory are commonly used to estimate the active lateral earth pressure. However, both of the theories assume the backfills can extend to a sufficient distance in which the failure plane can fully develop, so that these approaches cannot take account of the influence of the backfill width behind the wall [1, 2]. This is not a realistic case; in fact, more and more cases with narrow backfill width are considered in recent years; e.g., rock formations are close to the wall in mountain area [3–6], mechanically stabilized earth (MSE) walls built in front of previously stabilized walls in order to widen the existed highways for traffic [7–9], and the pit supporting structure built near the existing building in urban agglomeration areas, all as shown in Figure 1. In these cases, the narrow backfill has an obvious influence on the full development of a failure wedge when predicted by the Rankine theory or Coulomb's theory. It indicates the limitation of those methods in the utilization.

Furthermore, the discrepancy of the active earth pressure of narrow cohesionless backfill against rigid retaining walls is calculated by traditional theories, and the field data have been verified by centrifuge model tests. Frydman and Keissar [10] carried out a series of centrifugal model tests on rigid retaining walls with sand backfill to observe the changes in earth pressures behind the wall from at-rest conditions to active conditions. It is observed that the coefficient of active lateral earth pressure decreases with the depth and is smaller than the value calculated with the Rankine theory. Centrifugal tests [11] were carried out to investigate on the arching effects on unyielding retaining walls with narrow backfill width, while the lateral earth pressure acting on a retaining wall with narrow backfills is clearly smaller than the estimation based on the Rankine theory or Coulomb's theory. Afterwards, centrifugal model tests on reinforced soil walls adjacent to a stable face, conducted by Woodruff [12],

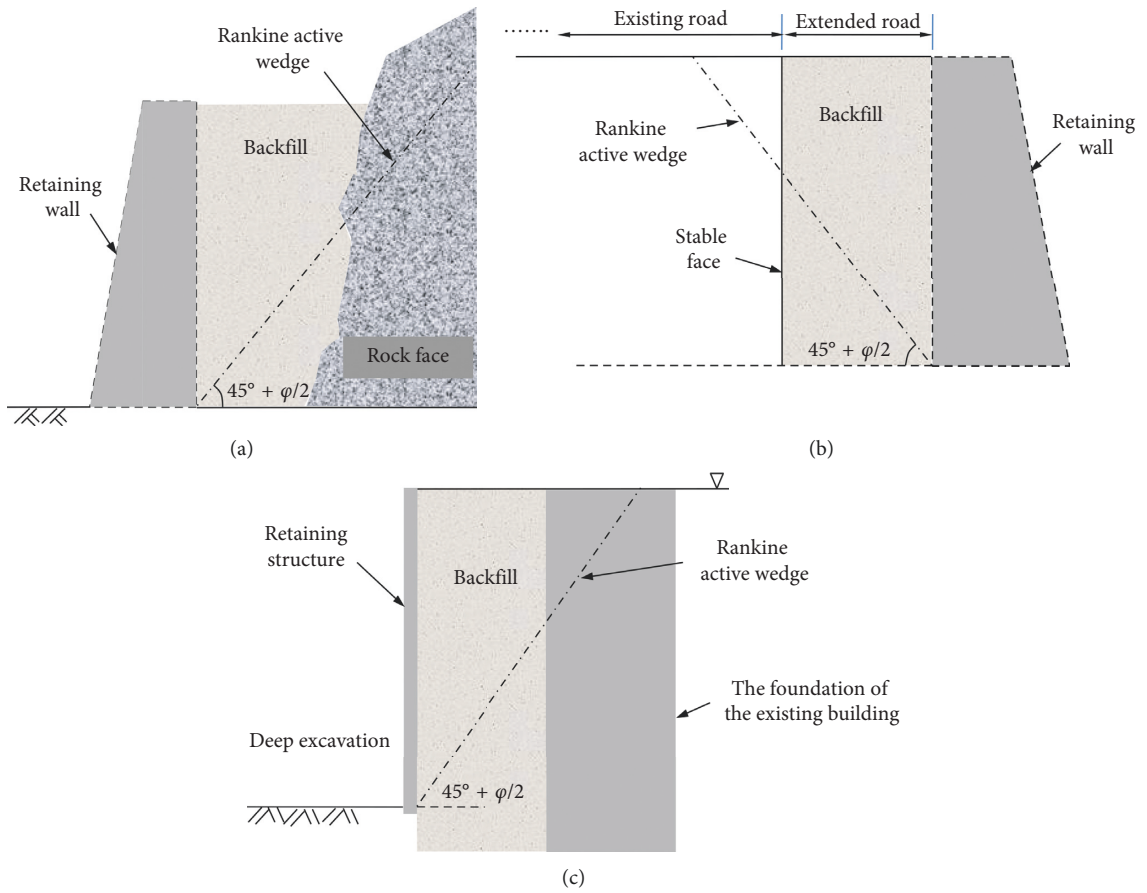

Figure 1: A schematic for narrow width soil behind a retaining wall: (a) near a rock; (b) near an existing road; (c) near an existing building.

indicate that the slip line of the backfill is bilinear rather than the linear failure plane with an inclination angle of $(45^\circ + \varphi/2)$ from the horizontal assumed by the Rankine theory, where φ is the internal friction angle of the soil. All these suggest that traditional methods that assume the Rankine failure plane to evaluate the active thrusts are not applicable for narrow walls, and an appropriate approach must be used.

As a consequence, some novel approaches should be provided for solving this problem. In this regard, numerical methods such as the finite element method (FEM), the discrete element method (DEM), and finite element limit analysis (FELA) were used to reveal the failure mechanic of the narrow backfill behind the retaining wall under more complex geometrical and geotechnical conditions in practice [4, 8, 13–15]. Taking the various geometries of the limited backfill space, Fan and Fang [4] found that the coefficients of the active earth pressure are considerably less than the Coulomb solution based on FEM, while the result of active earth pressure is generally located at locations higher than the lower one-third of the wall height. In addition, the instability mechanism of the backfill under constrained spaces was revealed, and the reduction factors of the active earth pressure had been also proposed based on FEM [8, 14] when the soil was reinforced. Li et al. [13] built a series of discrete element models with different soil widths to simulate the transition of the resultant lateral force and found that the resultant lateral force exerted on the wall decreases with the wall movement and eventually reaches a constant value. Chen et al. [15] explored the active earth pressure acting on the retaining wall of a narrow backfill under the translation mode using a finite element limit analysis. The results show that due to the boundary conditions, reflective shear bands occur in the backfill when it is failing.

However, the numerical method is seldom used because of its complexity; hence, many formulas deduced from analytical studies were proposed to satisfy the requirement of the practice engineers. Spangler and Handy [16] pioneered to develop an equation based on Janssen's arching theory [17] for calculating the lateral pressure caused by cohesiveness soil acting on the wall of a silo. Li and Aubertin [18] modified the Marston-based arching solution in order to consider the nonuniform distribution of the vertical stresses exerted on the walls retaining stope fills, and the pore pressure effects were further considered [18]. These studies found that the reason for the reduction of the lateral earth pressure acting on a retaining wall with narrow backfills is mostly due to soil arching effects. Additionally, taking the advantage of simplicity of the formulation, analytical solutions also have been derived for retaining walls with narrow backfills under the assumption that failure surfaces are planar and segmental [5, 19]. All these methods are useful for assessing the earth pressure for retaining walls with narrow backfills though with various degrees of approximation.

It is well worth pointing out that, in theoretical analyses, a reasonable assumption for the slip surface is fundamental to the study of active earth pressure. In this regard, many types of the planar slip surface have been proposed so far, such as lines (Coulomb and Rankine theory), segment lines [5, 19], circles [20], catenary lines [21], and curves composed of a line and a logarithmic spiral [22, 23]. Nevertheless, little attention in previous researches has been paid to the change of the slip surface, with which the narrow soil behind a retaining wall varies with the width of the backfill. To address this problem, the DEM was involved to analyze the exact slip surface shape of the soil behind a retaining wall with different aspect ratios of the limited backfill space. Additionally, a simple solution for evaluating the active earth pressure exerted by narrow backfill based on the exact slip surface, in terms of the limit equilibrium method, was presented. Meanwhile, the distribution, as well as the location of the resultant of active earth pressures, was also discussed in the paper.

2. Numerical Modeling by Using DEM and Verification

2.1. PFC-2D. Over the last few decades, the discrete element method (DEM) has been widely used by many researchers [24–29], especially in the study of particulate mechanics for macroscopic granular materials. The prime advantage of this method is its simplicity to simulate the interaction between granular particles and other boundaries, which means no description of the deformation behavior of granular materials itself is required. Furthermore, each distinct element is allowed to translate, rotate, and even arbitrarily separate to simulate the large deformation problems of granular soils caused by the movements of retaining wall. Therefore, the Particle Flow Code, *PFC-2D*/*3D*, based on the theory of DEM can be used to analyze the behavior of granular soils. It is well known that there are limitations when using the *PFC-2D* model when compared with the *PFC-3D* model, e.g., smaller number of particles and increasing arching effects in the simulation. Nevertheless, at present, it is still very usual to use the *PFC-2D* model to simulate behavior of granular soils, e.g., earth pressure [13, 30, 31], and these studies can obtain good simulation results. Herein, a numerical model established using the *PFC-2D* code program [32] was developed to investigate the behavior of narrow width soil behind a retaining wall, which was moved away from the soil gradually until reached the active state and formulated the final slip surface.

Unlike the analytical approach based on the continuous medium theory, the soil sample is assumed to be assembled by plenty of discrete rigid particles in *PFC-2D*, with which only the equilibrium equation of the element should be taken into account. Hence, the unbalanced forces or moments acting on the every particle will prompt it to move according to Newton's second law of motion, while the movement of each particle is affected by the resistance forces from other particles in contact as well. *PFC-2D* repeatedly utilizes explicit time-stepping successive cycles until the equilibrium equations for every single particle are satisfied. The forces and displacements of the particles are based on Newton's second law of motion and the contact forces based on the force-displacement law. Additionally, the macromechanical properties of granular soils and their contact will be determined by some micromechanical parameters, which are discussed subsequently in this study.

2.2. General Model for Soil behind Retaining Wall. The numerical model used for the failure mode of narrow cohesionless soil behind a retaining wall investigation is 9 m in height with upper 8.5 m-high section and the lower 0.5 m-high section, as shown in Figure 2. The lower section was fixed as the cushion layer for reducing boundary effects. The wall on the right is fixed to model the stationary wall and the left side wall moves away from the material, and the homogeneous soil was modeled as disc-shaped particles with radius ranging from 0.03 m to 0.05 m. Notice that the selected particles were chosen here just for saving computing time. To ensure the uniformity of the numerical specimens, the nine horizontal layers were prepared in this study. For each layer, a set of particles is first generated inside a box without contacting and then allowing them to move downward and come into contact with each other under gravity ($g = 9.81\ \mathrm{m/s^2}$), and the standard of the equilibrium state was the maximum contact force ratio reaching 0.001. Noted that all the wall elements are fixed, and the friction coefficient of the particle-wall interface is set to 0 during the sample preparation stage.

After the last layer reaching the equilibrium state, the friction coefficient of the particles was then increased to a maximum value, so as to compensate the lack of angularity for circular particles. The friction coefficient (μ_w) between the particles and the walls were kept constant during the whole process. Thus, the general calculated model was generated.

2.3. Material Properties. All the tiny particles, the rigid segments, and the contact between particles should be endowed some micromechanical parameters to reflect the known macromechanical properties. In this study, a linear contact stiffness model, governed by the value of normal and tangential stiffness, was used to describe the relationship between the force and displacement of each particle as well as the rigid segments. The parameters of stiffness and contact bond strength of the particles can be typically calculated by the following relationships [26, 32]:

$$\begin{aligned} k_s &= 1.2k_n, \\ k_n &= t \cdot E_c, \end{aligned} \tag{1}$$

where k_s is the tangential stiffness of the particles; k_n is the normal stiffness of the particles; t is the thickness of particles along the plane of paper with the default value 1.0 m; E_c, is the Young's modulus of the particle/particle contact.

Furthermore, in *PFC-2D*, some physical experiments at the macrolevel, e.g., biaxial test simulation, was also usually used to calibrate the micromechanical parameters of the particle mentioned before, i.e., k_s, k_n, and μ_s, and this approach was adopted in the present paper. Note that here the physical experiments are used for inversion of laboratory tests (e.g., triaxial test or direct shear test). Since the computational

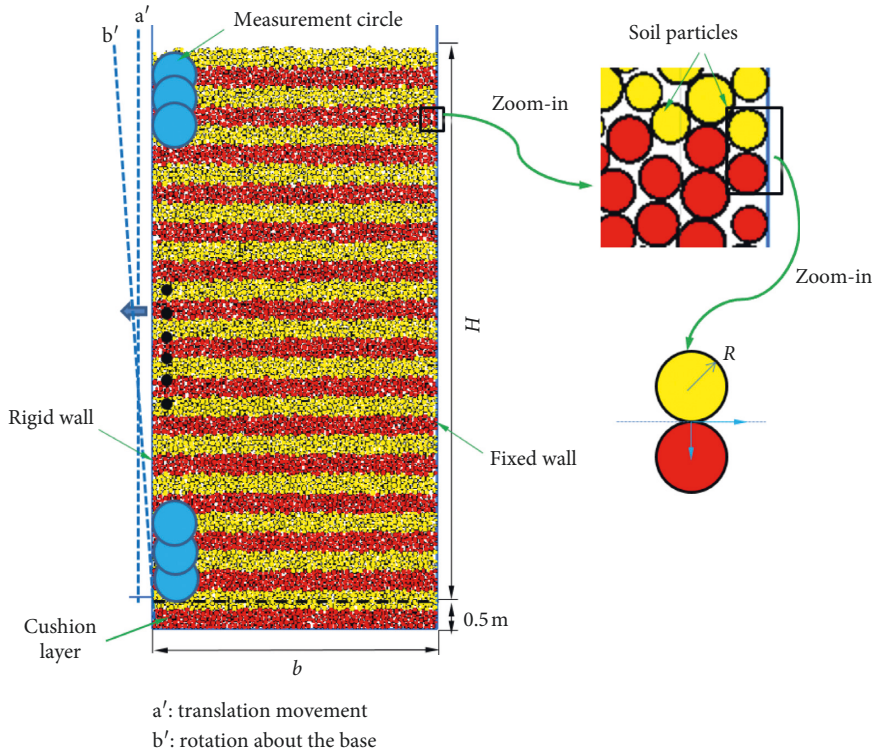

Figure 2: DEM model for soil behind a retaining wall.

time is highly depending on the particle numbers in DEM simulation, the "upscaling" technique of modeling particles was used here, which has been presented by many scholars [33–35]. As such, the biaxial sample with a width of 4.2 m and a height of 8.4 m generated in the same manner as mentioned above, herein, was used to calibrate the micromechanical parameters of soils, and the dimensions of the sample were determined by the data of a laboratory test in the previous literature [10], as a verified case discussed later.

The dimensions (width and height) of the biaxial sample were not realistic for a laboratory test; however, they were chosen to allow the generation of a sufficient number of particles (number of particles = 3,422) for the biaxial test simulation. The deviatoric stress versus the axial strain in the biaxial test with three different confining pressures (10 kPa, 20 kPa, and 40 kPa) is shown in Figure 3. The q-p' plot can be curved by the three Mohr's stress circle with different confining pressures. Therefore, the friction angle of the assembly defined as φ can be determined by the inclination angle of the q-p' line:

$$\frac{q}{p'} = \sin\varphi = 0.588, \tag{2}$$

where $\varphi = 36^{\circ}$, which was much smaller than the friction angle of the particle/particle contact. The micromechanical parameters governing the response of the materials at the macrolevel are presented in Table 1.

2.4. Estimation of the Active Earth Pressure along the Wall. As shown in Figure 2, the translational wall moves outward from the soil with a slight linear velocity (0.0001 m/s) which

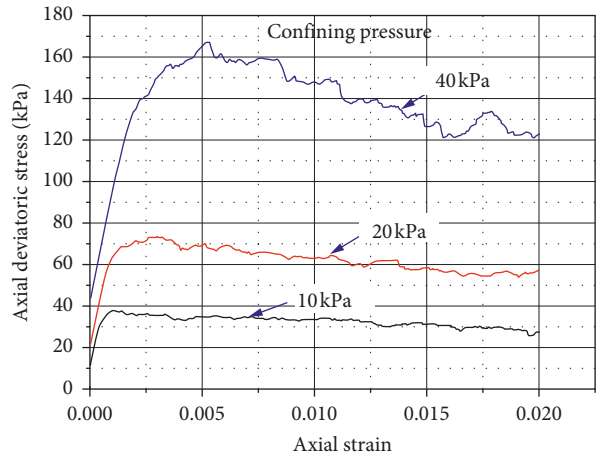

Figure 3: Deviatoric stress versus axial strain from PFC-2D biaxial test simulations.

can satisfy the quasi-static conditions and is close to the velocity adopted by Jiang et al. [30]. It was paused when displacement of the wall reached the 0.1 percent of the height of the wall. At this moment, the active earth pressure was assumed to occur [14]. However, the stress of the soil in DEM is discontinuous. Only the average contact stress between the particle and wall in a certain zone can be attained. Thus, the mean lateral stress acting on the wall in a certain zone was identified as the active earth pressure [32]. Furthermore, in total, twenty measurement circles with a radius of 0.4 m were arranged at the contact point closed to the removable wall from top to bottom as shown in Figure 2 to measure the mean lateral stress at the final stage of the simulation. Note that the above results were obtained after

Table 1: Micromechanical properties for the DEM analysis.

Parameter	Value
Soil	
Unit weight, γ	15.2 KN/m
Normal stiffness of particles, k_n	75 MN/m
Shear stiffness of particles, k_s	62.5 MN/m
Friction coefficient, μ_s	1.5
Particle radius, R	0.03–0.05 m
Retaining wall	
Normal stiffness of particles, k_n	2000 MN/m
Shear stiffness of particles, k_s	2000 MN/m
Friction coefficient, μ_w	1.0

the translational wall stopped moving, and the backfill reached the equilibrium state under gravity.

2.5. Validation. Frydman and Keissar [10] conducted a series of centrifuge tests to investigate the earth pressure acting on retaining walls near rock faces in active conditions, which were used as a classical verified example by many researchers [4, 8]. In the tests, the uniform fine sand with the particle size in the range of 0.1~0.3 mm, average unit weight (γ) of 15.2 kN/m^3, the relative density (D_r) of 70%, the internal friction angle (φ) of 36°, and interface friction angle (δ) of 25° was used as backfill materials. The micromechanical parameters are listed in Table 1. The retaining wall was made of wooden board with a height of 195 mm, which can simulate the similar stress level (43.7 g) for a full-scale wall with a height of 8.5 m. Some load cells were then arranged at the wall face near the top and bottom of the wall to capture the lateral pressure acting on the wall when the wall rotated around its base.

Figure 4 shows the comparison among the computed normalized active earth pressures (σ_x/γ_z) along the normalized depth from the DEM analyses, where z is the depth below the wall top and $b = 1$ m is the soil width, the theoretic solution based on arching equation [16], and the measured data from the centrifuge model wall test. Obviously, DEM simulation is in a good agreement with measurement, which means that DEM can simulate the distribution of the active earth pressure led by the movement of coarse-grain materials very well.

3. Analysis of the Failure Slip Surface Based on DEM

The typical model of the granular soil behind retaining walls considered in this study is shown in Figure 2. The height of the wall was kept as a constant value ($H = 8.5$ m), whereas the internal frictional angle of the soil (φ) varied from 20° to 45°. Furthermore, the movement of the wall was considered as horizontal translation only, and the other associated parameters used in the analysis are shown in Table 1.

In order to study the effect of the aspect ratio ($\beta = b/H$) of backfill on the failure model of the soil behind a rigid retaining wall, different widths (b) of the backfill were considered. Figure 5 shows the displacement field of the soil with different widths and a fixed internal friction angle value ($\varphi = 30°$) when the translation movement of the wall reaches

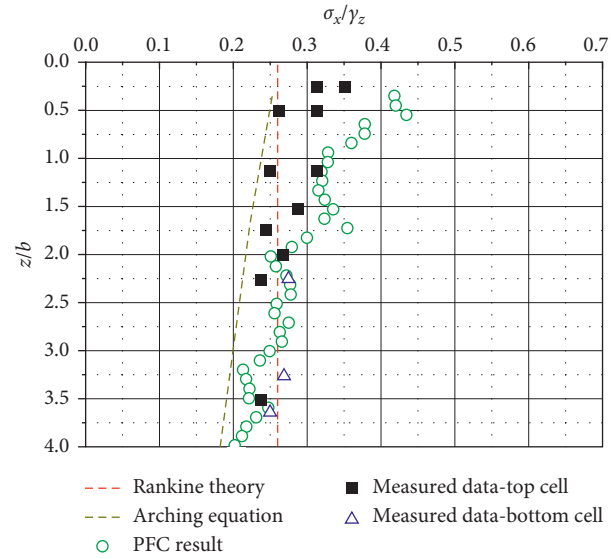

Figure 4: Comparison of the distribution of normalized active earth pressures (σ_x/γ_z) along normalized depth (z/b) among the PFC-2D results, experimental data, and theoretical solutions.

0.1 percent of the height of the wall. According to the Rankine and Coulomb theory, the minimum width of the backfill for active failure wedge that can be fully developed is easily calculated as 5.0 m and 5.889 m, respectively. Therefore, the widths of backfills are arranged in a range from 2.0 m to 8.0 m which are equivalent to the aspect ratio of the backfill, denoted as β, varies from 0.235 to 0.941.

The displacement field of the soil in the dark blue zone is almost close to zero, as illustrated in Figure 5, and this area can be identified as a stationary region when the wall moves, the similar way has been used by Nadukuru and Michalowski [29]. Therefore, the slip surface of the soil which is interpreted as the boundary between the static and moving soil can be approximately obtained with sufficient accuracy, while red lines were used to simulate the slipping of the soil with an inclination angle denoted as θ.

As can be seen in Figure 5, all the slipping lines are passing through the heel of the retaining wall to the top surface of the soil when the value of β meets the minimum distance requirement according to the Rankine theory (i.e., $\beta > 0.588$). However, with narrow backfill widths, partial failure surfaces were developed without passing through the heel of the retaining wall to the top surface of the soil. More particularly, with precise measurements, it is noted that the value of θ is kept as constant ($\theta = 60°$) regardless of the width of the backfill, which indicates that θ is almost independent of β.

For granular soil, the inclination angle of the slipping surface of the soil behind a retaining wall is only related to the internal friction angle based on the Rankine theory. The shape of the active failure wedge was also investigated with different φ which is on a scale from 20° to 35°, which covers the properties for most of the granular soil, as shown in Figure 6. According to the one-to-one relationship between φ and μ_s (friction coefficient of soil particles in *PFC-2D*), the targeted value of φ can be achieved by adjusting the value of μ_s.

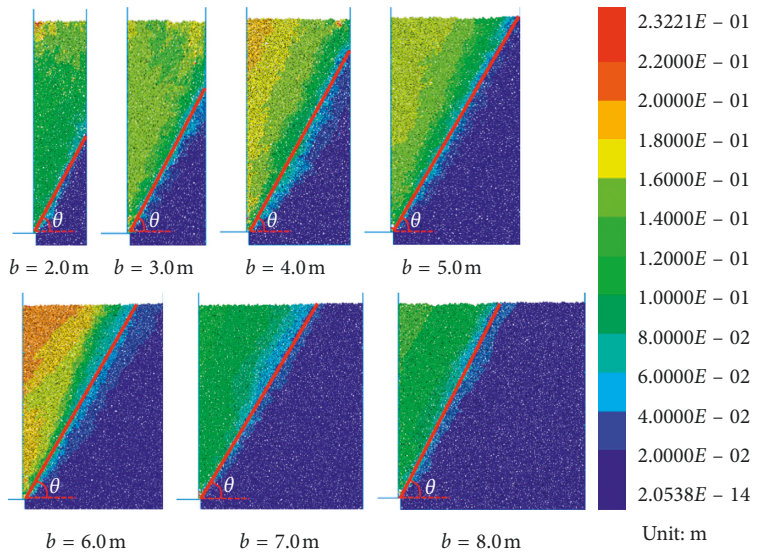

Figure 5: The slip surface of soil behind a retaining wall with widths varying from 2.0 m to 8.0 m ($\varphi = 30^{\circ}$).

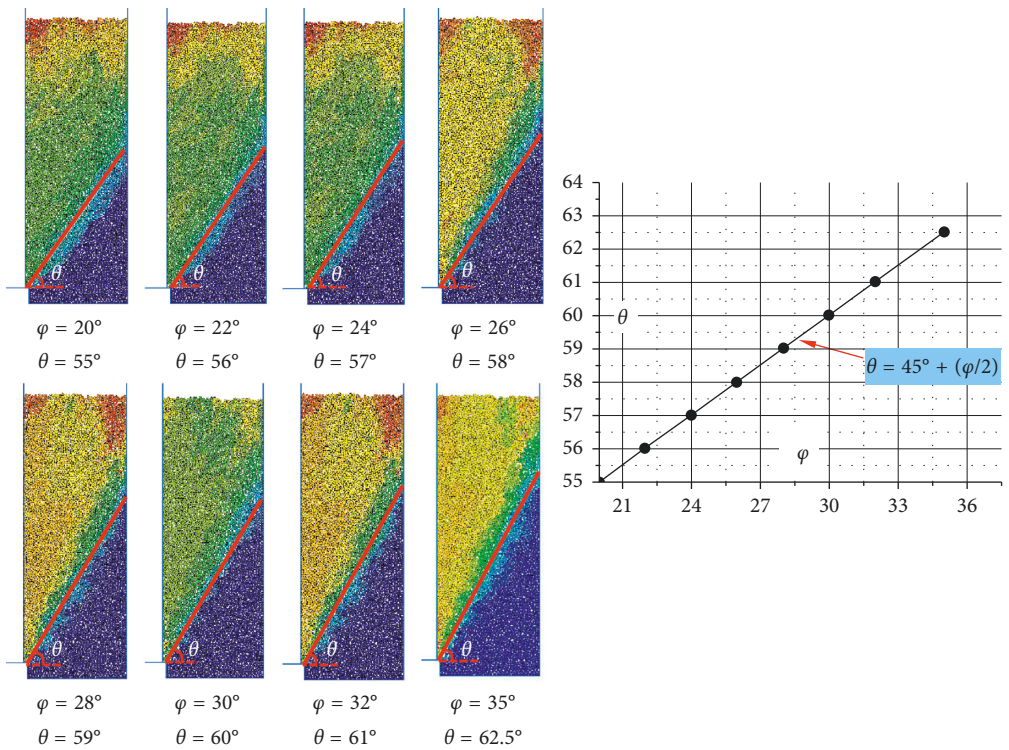

Figure 6: The slip surface of soil behind a retaining wall with φ varying from 20° to 35° ($d = 3$ m).

As can be seen from Figure 6, partial failure planar surfaces passing through the heel of the retaining wall can be still obtained with different values of φ whereas slight changes of the inclination angle of the slipping surface is observed. The relationship between the values of θ and φ is approximately linear and can be expressed as follows:

$$\theta = 45^{\circ} + \frac{\varphi}{2}. \tag{3}$$

Exact same relations can be obtained from the Rankine theory, which indicates that limited width of the backfill changes the length rather than the inclination angle of the active failure wedge. In other words, the two-dimensional section of the active failure wedge can be simplified as a trapezoid shape if the width of the backfill is less than the minimum distance, with which the active failure wedge can be fully developed. Therefore, a new method to calculate the

active earth pressure more reasonable in such case is required.

4. Simplified Analytical Approaches for Active Earth Pressure

The estimation of active earth pressures acting on the retaining wall is extremely important for geotechnical design, and analytical approaches are imperative for practical use. Due to the stress redistribution caused by soil arching phenomenon verified by many models and centrifuge tests, the classic Coulomb and Rankine active earth pressure theories usually underestimate the lateral pressure acting on retaining walls, especially when the backfill widths are narrow. As a result, Spangler and Handy [16] developed an analytical solution to simply calculate the lateral pressure acting on the wall of a silo, accounting for the possible soil arching in the backfill. By choosing an arbitrary horizontal slice element from the backfill with a depth z, confined by two rigid surfaces (Figure 7(a)), the vertical frictional forces at the interface between the backfill and the rigid surfaces will reduce the overall vertical stress together with the lateral pressure acting on the wall. The force equilibrium of the horizontal element in the vertical direction can be written as follows:

$$b\frac{d\sigma_z}{dz} + 2\tan\delta\sigma_x - \gamma b = 0, \tag{4}$$

where σ_z and σ_x are the vertical stress at depth z, respectively. Here, δ is the interface frictional angle between the backfill and the rigid wall, γ is the unit weight of the backfill, dz is the thickness of the horizontal element, and the earth pressure coefficient K is defined as the ratio of the horizontal stress σ_x over the vertical stress σ_z ($K = \sigma_x/\sigma_z$), which depends on the state of movement of the wall and material properties. In particular, for active pressure condition using the trigonometry of the Mohr's circle which represents the stress state of a soil element adjacent to the retaining wall (Figures 7(a) and 7(b)), under active conditions, the value of K can be derived as following equation [10]:

$$K = \frac{\left(\sin^2\varphi + 1\right) - \sqrt{\left(\sin^2\varphi + 1\right)^2 - \left(1 - \sin^2\varphi\right)\cdot\left(4\tan^2\delta - \sin^2\varphi + 1\right)}}{\left(4\tan^2\delta - \sin^2\varphi + 1\right)}. \tag{5}$$

The solution for the lateral active pressure at a given depth z can be obtained from the following equation:

$$\sigma_x = \frac{\gamma b}{2\tan\delta}\left[1 - \exp\left(-2K\frac{z}{b}\cdot\tan\delta\right)\right]. \tag{6}$$

However, arching equation pays no attention to the effect of the slip surface shape to the distribution of the lateral earth pressure acting on the retaining wall. This is because the soil slice element is identified as perfectly symmetrical with respect to the central line, and the research conducted herein aims to address this problem.

As mentioned before, the sliding surface of the narrowed soil behind the retaining wall was limited to a partial planar surface with an inclination angle dependent on the characteristic of the soil. Hence, the active earth pressure acting on the retaining wall with different depths accounting for the narrow width of the soil can be derived. The calculation model is schematically shown in Figure 8, where the trapezoid sliding soil block, denoted as ABCD, is divided into two parts. The active earth pressure along the wall herein can be obtained based on the conditions of equilibrium of forces acting on each wedge, AECD or EBD.

For an arbitrary horizontal thin-layer element within wedge AECD, all the external force is illustrated in Figure 8(b), and the equilibrium equation in the z-direction can be expressed as follows ($0 \le z \le H - b\cdot\tan\theta$):

$$\gamma b\cdot dz + \sigma_z b - \left(\sigma_z + d\sigma_z\right)b - 2\sigma_x\tan\delta\cdot dz = 0. \tag{7}$$

Similar to the derivation process of arching equation (Spangler and Handy, 1984), defining $\sigma_x = K\cdot\sigma_z$, where K is the coefficient of lateral pressure on the wall, is determined by equation (5). So equation (7) can be improved as follows:

$$\frac{d\sigma_z}{dz} = \gamma - 2K\cdot\sigma_z\tan\frac{\delta}{b}. \tag{8}$$

The differential equation can be solved accounting for the boundary condition at the top point of the soil ($z = 0$), where the vertical stress σ_z equals to zero:

$$\sigma_z = \frac{b\left(\gamma - \gamma\cdot e^{-2K\cdot z\cdot\tan\delta/b}\right)}{2K\cdot\tan\delta}. \tag{9}$$

And the lateral stress σ_x is thus given by the following equation:

$$\sigma_x = \frac{b\left(\gamma - \gamma\cdot e^{-2K\cdot z\cdot\tan\delta/b}\right)}{2\tan\delta}. \tag{10}$$

Similarly, according to the force analysis for an arbitrary horizontal thin-layer element within wedge EBD, the lateral thrust acting on the lower part of the wall is also deduced based on the equilibrium conditions of both directions, x and z directions. Under such a balanced force system, the applied forces acting on the wedge EBD can be simplified as two concentrated loads, i.e., normal force N and tangential force T along the sliding surface. Meanwhile, N and T satisfy a specific relationship, i.e., $T = N\tan\varphi$.

Therefore, for $\sum F_x = 0$, the equilibrium equation in the x-direction can be expressed as follows ($0 \le x \le b$):

$$\sigma_x + \frac{T}{\tan\theta} = R. \tag{11}$$

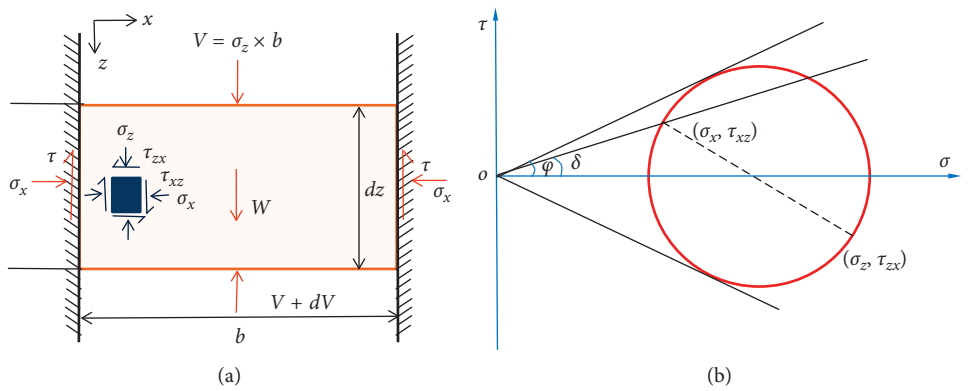

FIGURE 7: Force equilibrium analysis for slice element: (a) horizontal element of the backfill between two rigid faces and (b) stress conditions of a soil element adjacent to the back of retaining wall.

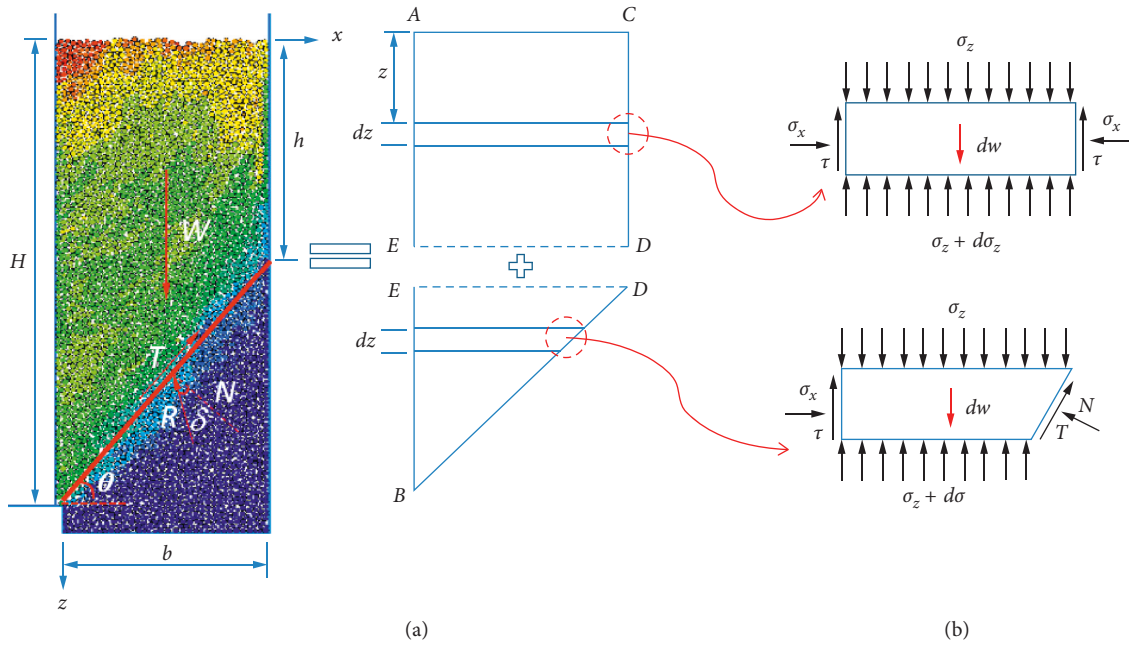

FIGURE 8: Schematics of calculation model: (a) block above the sliding surface and (b) analysis for thin-layer element.

Similarly, for $\sum F_z = 0$, the equilibrium equation in the x-direction can be expressed as follows ($H - b \cdot \tan\theta \le z \le H$), where the second-order small quantities are ignored:

$$\frac{d\sigma_z}{dz} = \gamma + \frac{\sigma_z - R - T\tan\theta - K\sigma_z \cdot \tan\delta \cdot \tan\theta}{H - z}. \tag{12}$$

Then, equation (11) can be substituted in equation (12) to obtain the following equation:

$$\frac{d\sigma_z}{dz} = \gamma + \frac{\sigma_z \cdot b_0}{H - z}, \tag{13}$$

where $b_0 = 1 - K(\tan\delta \cdot \tan\theta + \tan\theta + \tan\varphi \cdot \tan^2\theta / \tan\theta - \tan\varphi)$.

The lateral stress σ_x along the wall can be obtained by integrating equation (13) to obtain the following equation:

$$\sigma_x = K \cdot \frac{z - H}{b_0 + 1} \cdot \left\{ \gamma - \left[\frac{C_0}{(H - z)^2} \right]^{(b_0+1)/2} \right\}, \tag{14}$$

where C_0 is an integral constant which can be obtained by combining equations (10) and (14) with the same value of z ($z = h = H - b \cdot \tan\theta$), accounting for the continuous distribution conditions of the lateral stress along the wall.

Furthermore, by integrating equations (10) and (14) in terms of z along the wall, the resultant of active earth pressure acting on the rigid retaining wall can be obtained as follows:

$$E_h = \int_0^h \frac{b(\gamma - \gamma \cdot e^{-2K \cdot z \cdot \tan\delta / b})}{2\tan\delta} dz + \int_h^H K \cdot \frac{z - H}{b_0 + 1} \cdot \left\{ \gamma - \left[\frac{C_0}{(H - z)^2} \right]^{(b_0+1)/2} \right\} dz, \tag{15}$$

where E_h is the resultant of active earth pressure.

The total moment caused by active earth pressure to the heel of the retaining wall can be illustrated as follows:

$$M = \int_0^h \frac{b\left(\gamma - \gamma \cdot e^{-2K \cdot z \cdot \tan\delta / b}\right)}{2 \tan\delta} \cdot (H - z)dz + \int_h^H K \cdot \frac{z - H}{b_0 + 1} \cdot \left\{ \gamma - \left[\frac{C_0}{(H - z)^2} \right]^{(b_0+1)/2} \right\} \cdot (H - z)dz. \quad (16)$$

The distance from the location of the resultant of active earth pressures to the heel of the wall, denoted as h_0, can be easily derived as the ratio of M to E_h:

$$h_0 = \frac{M}{E_h}. \quad (17)$$

5. Comparison with Other Studies

The proposed new formulations for calculating the active earth pressure acting on the retaining wall with narrow backfill are applied to some previous model tests, which are well documented in the literature.

Case 1. The first laboratory test was conducted by Tsagareli [1], where the distribution of the active earth pressures acting on the translating rigid retaining wall with the height of 4 m and a width of 1.2 m for narrow backfill was measured. The other values of the parameters designed in the tests are given as follows: $\gamma = 17.658\,\text{kN/m}^3$, $\delta = 10^\circ$, and $\varphi = 37^\circ$. Figure 9 shows the comparison among the computed earth pressure along the retaining wall from the proposed equation, other theoretic solutions, and the measured data from the model test. As can be seen in Figure 9, the estimated values of earth pressure from the approach in this study show a good agreement with the measured data and provide a better prediction in comparison with other analytical solutions in the latter part of the curves, where the values of earth pressure decrease with the increase of depth. The phenomena have also been observed in other experiments [36, 37] and analytical solutions [38]. These results show the conventional approaches are overly conservative.

Case 2. A comparison is presented between the predictions of active earth pressure and the measured data due to a sand backfill behind a rigid wall in a laboratory test, which was reported by Fang and Ishibashi [36]. In the test, the active earth pressure distributions were observed with three different wall movement modes: (1) rotation about top, (2) rotation about heel, and (3) translation. The rigid wall used in the test had a height of 1.0 m and a width of 1.02 m, while the parameters of the backfill are designed as $\gamma = 15.4\,\text{kN/m}^3$, $\delta = 17^\circ$, and $\varphi = 34^\circ$. The active earth pressure versus the depth relationships from the measured and the predicted with the proposed and other previous approaches when the rigid wall translated are presented in Figure 10. The estimated active earth pressure based on the proposed method in this study is closer to the measured data than those obtained from other approaches, especially in the lower part of the wall. It is noted that the reduction of active earth pressure was not observed, which is partially due to enough width of the backfill preventing the formation of soil arching during the test.

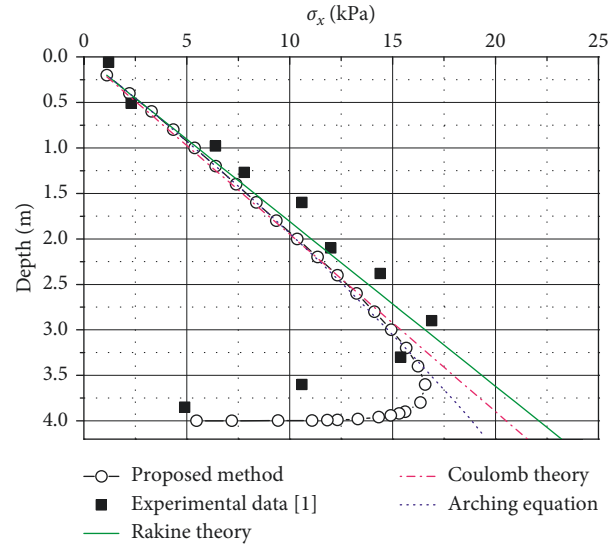

Figure 9: Comparison of the distribution of active earth pressures along depth between the theoretical solution and experimental data [1].

6. Parameter Analysis

In addition, the effects of some prime parameters, such as the width of the backfill, internal friction angle of soil, and wall-soil friction angle on the distribution of active earth pressure, are further analyzed, in which the basic parameters are given as follows: $H = 8.5$ m, $b = 3.0$ m, $\gamma = 18.0\,\text{kN/m}^3$, $\delta = 20^\circ$, and $\varphi = 30^\circ$.

Figure 11 shows the lateral active earth pressure distribution along the height of a translating rigid wall for the various widths of backfill (the value of b is in the range from 1.0 m to 5.0 m, in which the value of aspect ratio of the backfill is from 0.117 to 0.588). As shown in Figure 11, the magnitude of the active earth pressure decreases with the decrease of the backfill widths, and the attenuation becomes clearer when b value is smaller. It can be explained that the width of the narrow backfill plays an important role in the development of arching in the backfill, and the arching effect can be strengthened with the narrower distance between the retaining wall and the existed rigid wall by undertaking more self-weight of the soil.

In order to study the effect of the soil internal friction angle (φ) and wall-soil friction angle (δ) on the lateral active earth pressure against the rigid, various values of φ varying from 24° to 35° and δ varying from 6° to 20° were employed. The change of active earth pressure along the height of the wall is shown in Figures 12 and 13. As seen in Figures 12 and 13, a clear similar trend is observed with different values of φ and δ. This indicates that those two parameters influence the magnitude of the active earth pressure significantly but not the shape of its distribution. In particular, the values of earth pressure increase with the increasing φ value, whereas

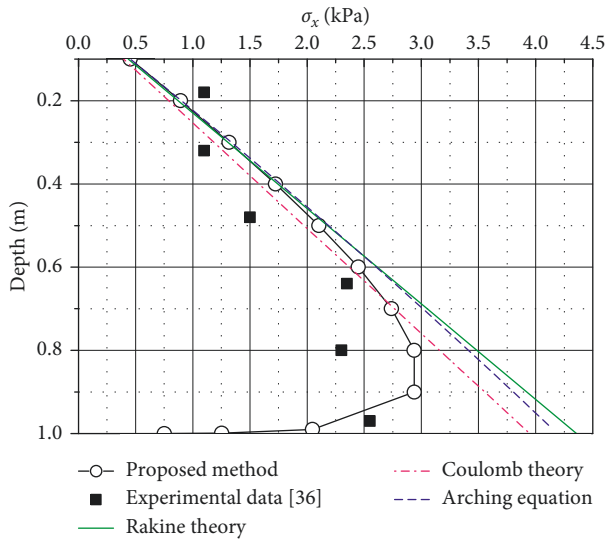

Figure 10: Comparison of the distribution of active earth pressures along depth between the theoretical solution and experimental data [36].

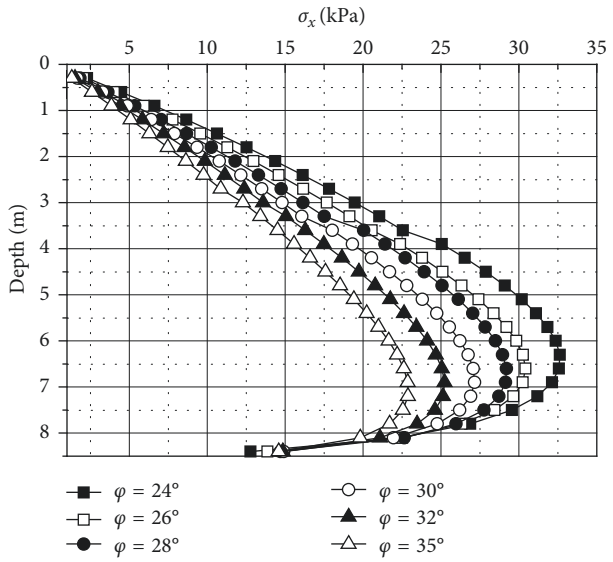

Figure 12: Variation of the active earth pressures along the length of the retaining wall at various internal friction angles of soil (φ).

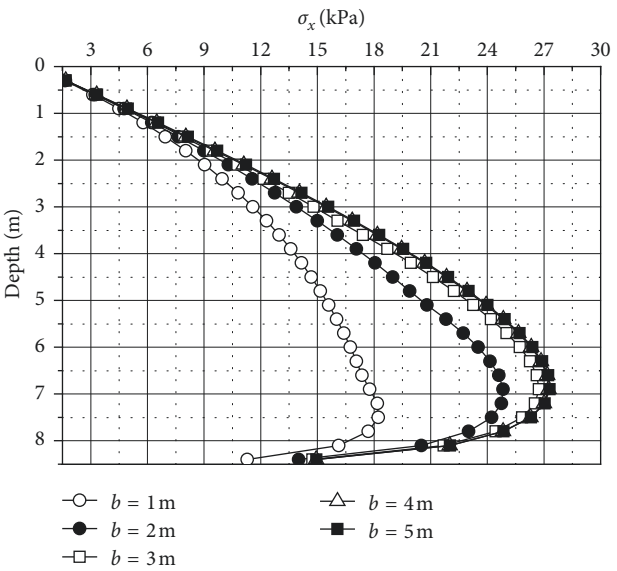

Figure 11: Variation of the active earth pressures along the length of the retaining wall at various fill widths.

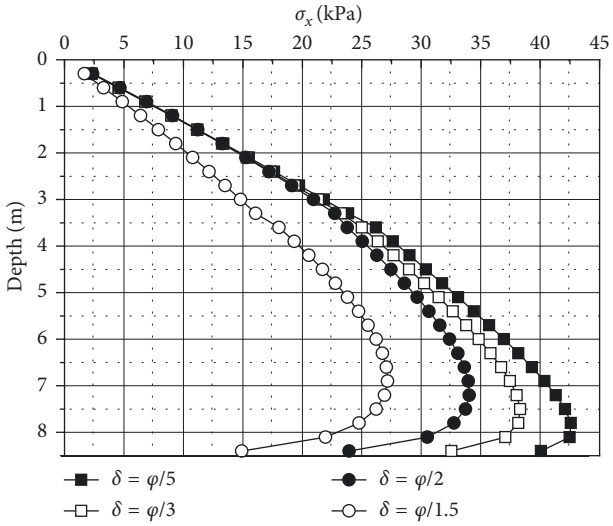

Figure 13: Variation of the active earth pressures along the length of the retaining wall at various wall-soil friction angle of soil (δ).

decrease with the value of δ owing to the reduction of the wall-soil interaction supporting the self-weight of the soil.

It is widely accepted that the height, where the lateral resultant active force is applied, normalized by wall height (h_0/H) maintains one-third according to the Rankine theory and Coulomb theory because of the triangular distribution of the active earth pressure along the retaining wall. However, the calculations for active earth pressure based on the Rankine theory and Coulomb theory ignore the effect of the width of the backfill. The point of application of the resultant active earth pressure is also investigated in this study.

As can be seen in Table 2, b varies from 2.0 to 4.0, by using the present approach. Only slight changes of h_0/H can be observed, and the approximate h_0/H value is regarded as 0.38, which is closer to the measured data from experiments than the computed value based on the Rankine theory and Coulomb theory.

Figure 14 shows the variation of the location (h_0/H) of the resultant of active earth pressures with the different internal frictional angles of soil and wall-soil frictional angle. The locations of the resultant of active earth pressures decrease with the increase of φ values, while increases with the increase of δ values. For a φ value varying from 22° to 38°, a decrease of the h_0/H value from 0.408 to 0.368 can be achieved. Whereas the h_0/H value will increases from 0.344 to 0.380 when the φ value varies from 6° to 20°. In general, the h_0/H value is basically in a range of 0.34 to 0.40, and this is significantly higher than one-third of the wall height.

Table 2: Variation of the location of the resultant (h/H) of active earth pressures with various fill widths.

Methods	b					Average
	2.0 m	2.5 m	3.0 m	3.5 m	4.0 m	
Coulomb theory	0.33	0.33	0.33	0.33	0.33	0.33
Experimental study [1]	0.43	0.42	0.43	0.41	0.41	0.42
Presented approach	0.391	0.380	0.392	0.371	0.372	0.381

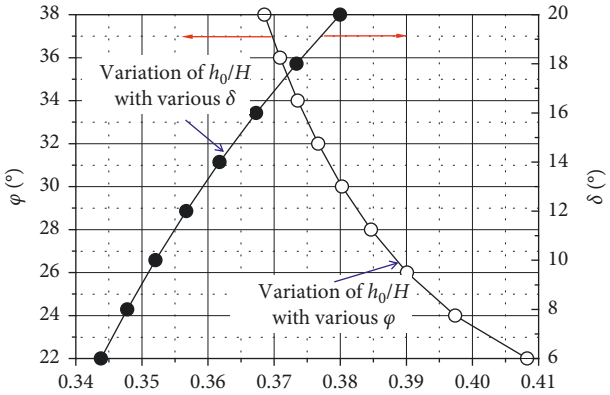

Figure 14: Variation of the location of the resultant (h_0/H) of active earth pressures with different internal frictional angles of soil (φ) and wall-soil frictional angle (δ).

7. Conclusions

The estimation of active earth pressures acting on the retaining wall is extremely important for geotechnical design, and its rationality depends on the accuracy of the simulated failure model of the soils. Compared to the conventional approach, such as the Rankine or Coulomb theory, which is suitable only for the retaining walls with narrow width of the backfills, this study presented a new simplified method using limit equilibrium analysis for determining the nonlinear distribution of the active earth pressure on rigid retaining walls with limited backfills. This new approach is based on the horizontal thin-layer element method and the exact slip surface shape that was determined by the DEM simulation (*PFC-2D*). A good agreement can be obtained between the proposed method and experimental results. In addition, the effect of the aspect ratio of the backfill width and the friction angle of the backfill on the distribution of active earth pressures along the wall was also discussed. The main features of this study are summarized below:

(1) The two-dimensional section shape of the active failure wedge of the backfill with a limited width can be confirmed as a trapezoid composed of an upper rectangle part and a lower triangle part. The inclination angle of the triangle failure wedge is related to the value of the internal friction angle of the soils;

(2) The lateral active earth pressure decreases significantly with the decrease of the width of the backfill, which indicates that the soil arching plays a more important role with narrower width of the backfill.

(3) The point of active earth pressures is noticeably higher than one-third of the wall height described in the Rankine and Coulomb theory.

Data Availability

The data used to support the findings of this study are available from the corresponding author upon request.

Conflicts of Interest

The authors declare that there are no conflicts of interest.

Acknowledgments

The authors would like to acknowledge the financial support from the National Science Foundation of China under contract no. 51278184.

References

[1] Z. V. Tsagareli, "Experimental investigation of the pressure of a loose medium on retaining walls with a vertical back face and horizontal backfill surface," *Soil Mechanics and Foundation Engineering*, vol. 2, no. 4, pp. 197–200, 1965.

[2] X. L. Yang and J. H. Yin, "Estimation of seismic passive earth pressures with nonlinear failure criterion," *Engineering Structures*, vol. 28, no. 3, pp. 342–348, 2006.

[3] S. G. Lee and S. R. Hencher, "The repeated failure of a cut-slope despite continuous reassessment and remedial works," *Engineering Geology*, vol. 107, no. 1-2, pp. 16–41, 2009.

[4] C. C. Fan and Y. S. Fang, "Numerical solution of active earth pressures on rigid retaining walls built near rock faces," *Computers and Geotechnics*, vol. 37, no. 7-8, pp. 1023–1029, 2010.

[5] J. J. Chen, M. G. Li, and J. H. Wang, "Active earth pressure against rigid retaining walls subjected to confined cohesionless soil," *International Journal of Geomechanics*, vol. 17, no. 6, article 06016041, 2016.

[6] M. H. Yang and X. Tang, "Rigid retaining walls with narrow cohesionless backfills under various wall movement modes," *International Journal of Geomechanics*, vol. 17, no. 11, article 04017098, 2017.

[7] K. T. Kniss, K. H. Yang, S. G. Wright, and J. G. Zornberg, "Earth pressures and design consideration of narrow MSE wall," in *Proceedings of the Texas Section ASCE Spring*, ASCE, Reston, VA, USA, 2007.

[8] K. H. Yang and C. N. Liu, "Finite-element analysis of earth pressures for narrow retaining walls," *Journal of Geo-Engineering*, vol. 2, no. 2, pp. 43–52, 2007.

[9] K. H. Yang, J. Ching, and J. G. Zornberg, "Reliability-based design for external stability of narrow mechanically stabilized earth walls: calibration from centrifuge tests," *Journal of Geotechnical and Geoenvironmental Engineering*, vol. 137, no. 3, pp. 239–253, 2011.

[10] S. Frydman and I. Keissar, "Earth pressure on retaining walls near rock faces," *Journal of Geotechnical Engineering*, vol. 113, no. 6, pp. 586–599, 1987.

[11] W. A. Take and A. J. Valsangkar, "Earth pressures on unyielding retaining walls of narrow backfill width," *Canadian Geotechnical Journal*, vol. 38, no. 6, pp. 1220–1230, 2001.

[12] R. Woodruff, "Centrifuge modeling of MSE-shoring composite walls," Master thesis, Department of Civil Engineering, The University of Colorado, Boulder, CO, USA, 2003.
[13] M. G. Li, J. J. Chen, and J. H. Wang, "Arching effect on lateral pressure of confined granular material: numerical and theoretical analysis," *Granular Matter*, vol. 19, no. 2, 2017.
[14] D. Leshchinsky, Y. Hu, and J. Han, "Limited reinforced space in segmental retaining walls," *Geotextiles and Geomembranes*, vol. 22, no. 6, pp. 543–553, 2004.
[15] F. Q. Chen, Y. J. Lin, and D. Y. Li, "Solution to active earth pressure of narrow cohesionless backfill against rigid retaining walls under translation mode," *Soils and Foundations*, 2018, in Press.
[16] M. G. Spangler and R. L. Handy, *Soil Engineering*, Harper and Row, New York, NY, USA, 1984.
[17] H. A. Janssen, "Versuche uber getreidedruck in silozellen," *Zeitschrift des Vereines Deutscher Ingenieure*, vol. 39, pp. 1045–1049, 1895.
[18] L. Li and M. Aubertin, "An analytical solution for the nonlinear distribution of effective and total stresses in vertical backfilled stopes," *Geomechanics and Geoengineering*, vol. 5, no. 4, pp. 237–245, 2010.
[19] V. Greco, "Active thrust on retaining walls of narrow backfill width," *Computers and Geotechnics*, vol. 50, pp. 66–78, 2013.
[20] W. F. Chen and N. Snitbhan, "On slip surface and slope stability analysis," *Soils and Foundations*, vol. 15, no. 3, pp. 41–49, 1975.
[21] R. L. Handy, "The arch in soil arching," *Journal of Geotechnical Engineering*, vol. 111, no. 3, pp. 302–318, 1985.
[22] J. Kumar, "Seismic passive earth pressure coefficients for sands," *Canadian Geotechnical Journal*, vol. 38, no. 4, pp. 876–881, 2001.
[23] K. S. Subba Rao and D. Choudhury, "Seismic passive earth pressures in soils," *International Journal of Geotechnical Engineering*, vol. 131, no. 1, pp. 131–135, 2005.
[24] P. A. Cundall and O. D. L. Strack, "A discrete numerical model for granular assemblies," *Géotechnique*, vol. 29, no. 1, pp. 47–65, 1979.
[25] C. Thornton, "Numerical simulations of deviatoric shear deformation of granular media," *Géotechnique*, vol. 50, no. 1, pp. 43–53, 2000.
[26] D. O. Potyondy and P. A. Cundall, "A bonded-particle model for rock," *International Journal of Rock Mechanics and Mining Sciences*, vol. 41, no. 8, pp. 1329–1364, 2004.
[27] L. Cui, C. O'Sullivan, and S. O'Neill, "An analysis of the triaxial apparatus using a mixed boundary three-dimensional discrete element model," *Géotechnique*, vol. 57, no. 10, pp. 831–844, 2007.
[28] J. Han, A. Bhandari, and F. Wang, "DEM analysis of stresses and deformations of geogrid-reinforced embankments over piles," *International Journal of Geomechanics*, vol. 12, no. 4, pp. 340–350, 2012.
[29] S. S. Nadukuru and R. L. Michalowski, "Arching in distribution of active load on retaining walls," *Journal of Geotechnical and Geoenvironmental Engineering*, vol. 138, no. 5, pp. 575–584, 2012.
[30] M. Jiang, J. He, J. Wang, F. Liu, and W. Zhang, "Distinct simulation of earth pressure against a rigid retaining wall considering inter-particle rolling resistance in sandy backfill," *Granular Matter*, vol. 16, no. 5, pp. 797–814, 2014.
[31] Y. Gao and Y. H. Wang, "Experimental and DEM examinations of K_0 in Sand under different loading conditions," *Journal of Geotechnical and Geoenvironmental Engineering*, vol. 140, no. 5, article 04014012, 2014.
[32] Itasca Consulting Group, *PFC2D Theory and Background*, Itasca Consulting Group, Inc., Minneapolis, MN, USA, 2004.
[33] Y. H. Wang and S. C. Leung, "A particulate-scale investigation of cemented sand behavior," *Canadian Geotechnical Journal*, vol. 45, no. 1, pp. 29–44, 2008.
[34] V. D. H. Tran, M. A. Meguid, and L. E. Chouinard, "A finite-discrete element framework for the 3D modeling of geogrid-soil interaction under pullout loading conditions," *Geotextiles and Geomembranes*, vol. 37, pp. 1–9, 2013.
[35] Z. Wang, F. Jacobs, and M. Ziegler, "Visualization of load transfer behaviour between geogrid and sand using PFC2D," *Geotextiles and Geomembranes*, vol. 42, no. 2, pp. 83–90, 2014.
[36] Y. S. Fang and I. Ishibashi, "Static earth pressures with various wall movements," *Journal of Geotechnical Engineering*, vol. 112, no. 3, pp. 317–333, 1986.
[37] Z. C. Tang, "A rigid retaining wall centrifuge model test of cohesive soil," *Journal of Chongqing Jiao tong University*, vol. 25, no. 2, pp. 48–56, 1988, in Chinese.
[38] K. H. Paik and R. Salgado, "Estimation of active earth pressure against rigid retaining walls considering arching effects," *Géotechnique*, vol. 53, no. 7, pp. 643–653, 2003.